Microsoft

Bifacial Cold plates for High Powered Servers

SU(Syracuse) Team: Evan Tulsky, Matthew MacFarlane, Jeremy Kang, Shalabh Maroo (Advisor)

Microsoft Team: Kathryn Oseen-Senda, Courtney Huddleston, Jorge Juarez, Martha Peterson, James Sun, Shaun Harris, Oscar Farias Moguel

Table of Contents

1 Abstract

As high-powered servers generate more heat, cooling becomes crucial. Traditional methods struggle, so a new solution using bifacial cold plates is explored. These plates use both sides to maximize cooling. The cold plate is cooled by water. Through simulations and testing, the thermal properties of the design are optimized, and materials are chosen with considerations to manufacturing restrictions. Our results show significant temperature reductions, ensuring stable server performance. This innovation offers a promising solution for cooling challenges in modern server systems.

As part of the senior capstone for mechanical engineering, the students are put in groups of about 3 or 4 to make 19 different groups and they are given a company sponsor based on their desires. This year, we got matched up with the Microsoft group and we were given the task to create a bifacial cold plate for a high-powered server.

2 Introduction

A significant amount of energy used at a data center is used for cooling. With increased computing demands, mechanical systems must ensure adequate cooling methods to protect equipment. Liquid cooling methods are proven to be a more efficient cooling method in servers and computers. The fans dissipating the heat into the air in the servers can lead to a slow build up in heat, which may lower efficiency, therefore a water-cooled system can dissipate the heat outside. Water also has a higher thermal conductivity and specific heat capacity than ambient air conditions. Thus, the transition to a liquid-cooled server can meet the increased power demands by converting from 600W chips being cooled by an air-cooled system to a desired 1000W chips. However, designs can be troubled with repairs due to additional design complexities and the potential of exposing electronics to liquid. Liquid leaking can be a major problem and can cause severe damage to the electronic surroundings, which all are added costs of using liquid coolers. Setting up a liquid cooling system may also lead to an increase in the total cost of liquid coolers due to the complex nature of installing a good system that will dissipate heat efficiently. Nevertheless, increased thermal removal to enable increased power supplies outweighs many other factors.

The development of a liquid cooled server is explored to provide efficient and adequate heat transfer from protected and stressed equipment. Heat is generated from the CPU (Central Processing Unit). Thus, special considerations are concerned with the CPU unit, but failure points persist on multiple aspects of design. Through numerous conduction processes, heat is moved from the CPU to the thermal interface material 2 (TIM2). Removed heat is removed from the system through convection of air or water from the cold plate and is dispersed to the surrounding atmosphere. The heat transfer pathway can be modeled in Figure 1.

Figure 1: *Path of Heat Transfer*

3 Design Approach

A microchannel design for the topside and bottom side of a server chip is designed and represented below with the green part of the design representing the entire motherboard. A constant heat flux is produced by a server chip in between the two microchannels such that the top surface of the microchannels is insulated. In this chapter, varying fin geometries are explored. Further, an ideal cold plate design utilizing copper is compared to brass considering the feasibility of design characteristics in different machining methods.

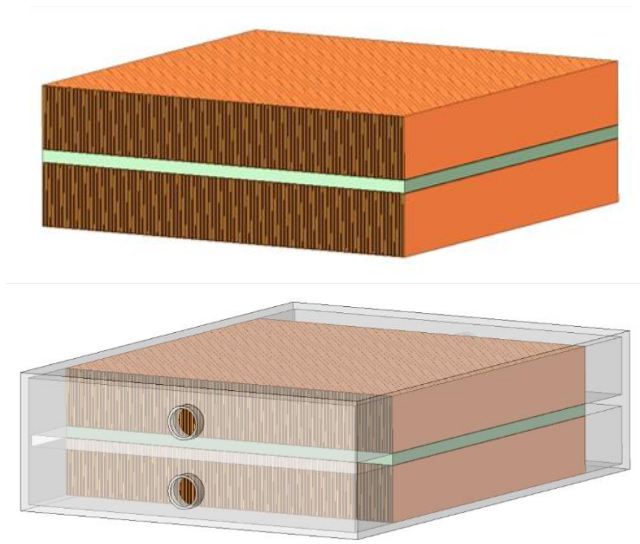

Figure 2: *Bifacial cold plate Designs with and without a manifold*

Design Constraints

The outcome of our system is to design a cooling system on a bifacial server chip to satisfy thermal and mechanical goals concurrently. The top surface consists of a single 1000W 50mm-by-50mm CPU server chip. The bottom side of the motherboard consists of 14 chips that produce a total of 112W with each chip being limited to a size of 8mm-by-8mm each. In subsequent analysis, the geometry of the chips is ignored and a single 112W of a size of 50mm-by-50mm is assumed. The design is expected to be able to be scaled up in total power output in future iterations of high-powered servers while continuing to deliver adequate cooling. The flow velocity can range from 1.0 to 2.5 liters per minute. The target range is 1.5 lpm per kW.

Design Specifications for the top surface (1000W chip)

- CPUs cooled below an operational case temperature of 80°C.

- The cooling system is to remain between a total case height of 48 mm.
- A cold plate no larger than 65mm-by-65mm.
- The inlet water temperature is 40°C.
- The target flow velocity = 1.5 lpm.
- A pressure drop < 1bar.
- A minimal wall thickness > 100 microns.

Design Specifications for the top surface (112W chip)

- CPUs cooled below an operational case temperature of 85°C.
- The cooling system is to remain between a total case height of 48 mm.
- A cold plate no larger than 65mm-by-65mm.
- The inlet water temperature is 40°C.
- The target flow velocity = 0.16 lpm.
- A pressure drop < 1bar.
- A minimal wall thickness > 100 microns.

Generation of Mathematical Models

Microchannels experience laminar flow in internal flow as the Reynolds Number is significantly below 2000. This results in a constant Nusselt number determined by the dimension ratio of the channel height and width. Using a constant heat flux and exploiting a high dimension ratio of the channel width and height greater than 8, the Nusselt number reaches a maximum value of 8.24 as seen in the chart below.

Channel width / height	Nu of constant heat flux	Friction factor, f
1	3.61	59.92/Re
2	4.12	62.20/Re
3	4.79	68.36/Re
4	5.33	72.92/Re
6	6.05	73.80/Re
8	6.49	82.32/Re
∞	8.24	96.00/Re

Figure 3: *Laminar flow of an internal rectangular channel chart*

As a result, the heat transfer coefficient, $h = \frac{Nuk_{water}}{D_h}$, is maximized with higher dimension ratios and can be further increased with smaller width and height dimensions from an effective hydraulic diameter, D_h. The resistance network of the heatsink consists of conduction and convection heat transfer such that convection is found to be a magnitude greater. Thus, increasing h significantly improves the thermal efficiency of the system. The total resistance, $R_{total} = \frac{H-\frac{h}{2}}{k_{cp}SW} + \frac{1}{\eta h A_t}$, can be utilized to find the surface temperature of the cold plate, $\frac{T_s-T_e}{T_s-T_i} = e^{\frac{-1}{\dot{m}c_p R_{total}}}$. Finally, the operating case temperature of the CPU is an additional conduction process of the integrated heat spreader (IHS) such that, $T_{case} = T_s + \frac{\dot{q}}{k_{IHS}L_{IHS}}$. Consequently, the pressure drop of the channels inlet and outlet flow grows exponentially from decreased channel dimensions. This is a result of an increased friction factor, f, increased squared average velocity derived from the cross-sectional area, and a decreased hydraulic diameter. This equation is modeled through $\Delta P = \frac{fW_{plate}v^2}{2D_h}$.

Generation of Preliminary Models

Initial cold plate designs explored the differences in geometric cross-sectional channels. Circular geometries were explored to minimize the effects of a formed boundary layer. However, square channels maximized cross sectional area and resulted in an increased total mass flowrate and were deemed more efficient. The different geometry can be seen in Figure 14. Simulations and calculations computed on the initial designs can be found in Figure 15 and it was found that the design can be optimized.

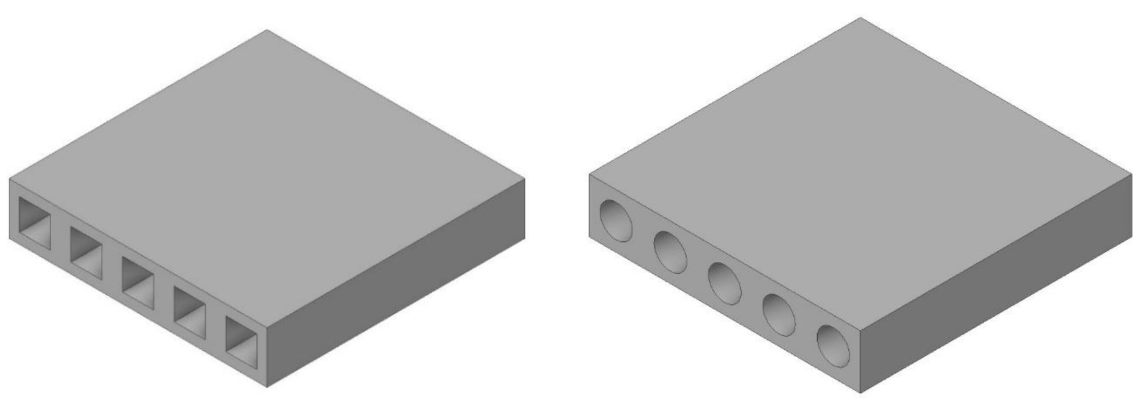

Figure 4: *Initial research designs. The left are square channels and right are circular channels.*

4 Advanced Modeling and System Simulation

In this chapter, a parametric analysis of the cross-sectional dimensions was computed following design specifications in Section 4-A. Simulations were performed on the optimal theoretical design for the top side and bottom side. Adhering to budget constraints and resources in house, a second design made of brass that is manufactured from CNC methods for testing in subsequent chapters.

Generation and Optimization of Models

I) Cold plate design using copper

The cold plate is made from copper material and designed to be manufactured utilizing skiving method. A parametric table analyses the case temperature, T_{case}, and pressure drop, ΔP, over changing wall thickness and channel length as derived in Section 3-B. Since heat is produced on from one side, it was determined that numerous vertical channels were inefficient to heat removal. The total height of both heat sinks is chosen to 10 mm. In the top surface cold plate in Figure 16, The cold plate provides cooling below the 80-degree case temperature limit when the channel width is below 1.38 mm assuming the heatsink for the 1000W CPU experiences an inlet temperature of 40 Celsius and 1.5 liters per minute.

The chosen top surface design includes one vertical channel such that the channel height is 9.64 mm. At channel widths near 0.1 mm, the case temperature of the CPU minimally decreases because of the asymptotic nature of the exponential term. Thus, the channel width is chosen as 200 microns with a wall thickness of 400 microns.

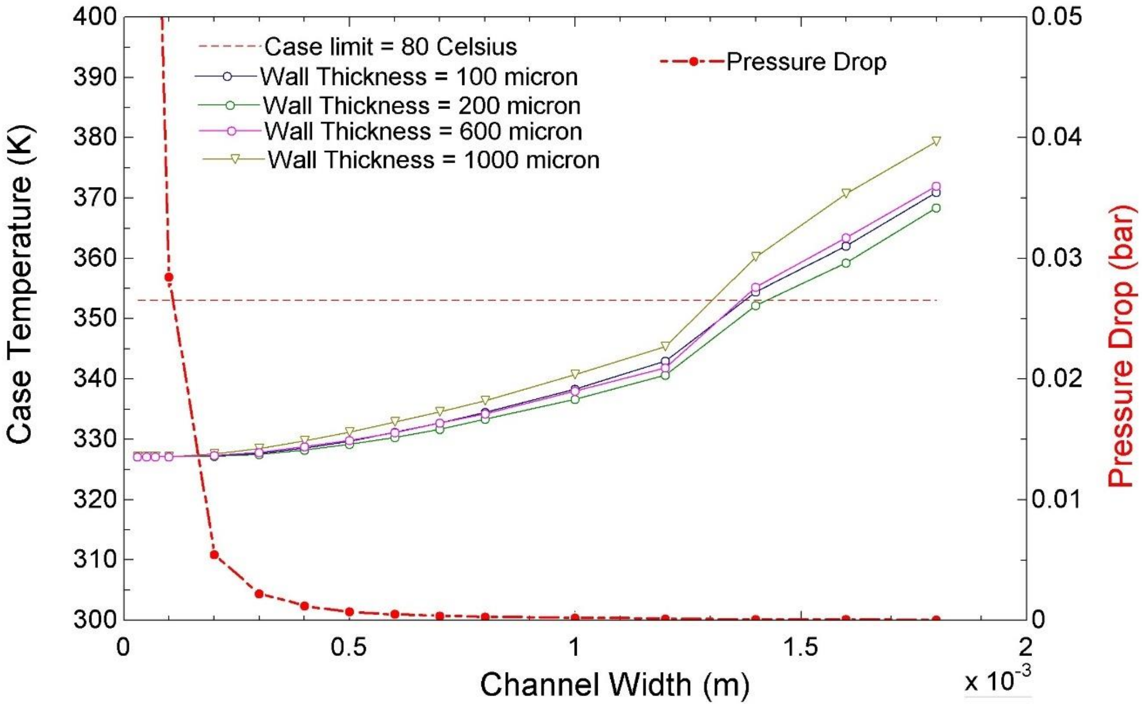

Figure 5: *Plot for Channel Dimensions vs Surface Temperature (top side)*

In the bottom surface cold plate in Figure 5, The cold plate provides cooling below the 85-degree case temperature limit when the channel width is below 3.50 mm assuming the heatsink for the 112W CPU experiences an inlet temperature of 40 Celsius and 0.16 liters per minute. Due to the decreased flowrate, the pressure drop remains smaller due to the squared velocity term as derived in Section 3-B. While the backside channel removes heat from a smaller power source, the target flow rate is significantly smaller requiring similarly small dimensions. The channel width is chosen as 800 microns and the wall thickness to be 200 microns. The total height of the backside channel is limited to 10 mm and one vertical channel is chosen such that the channel height is 9.64 mm.

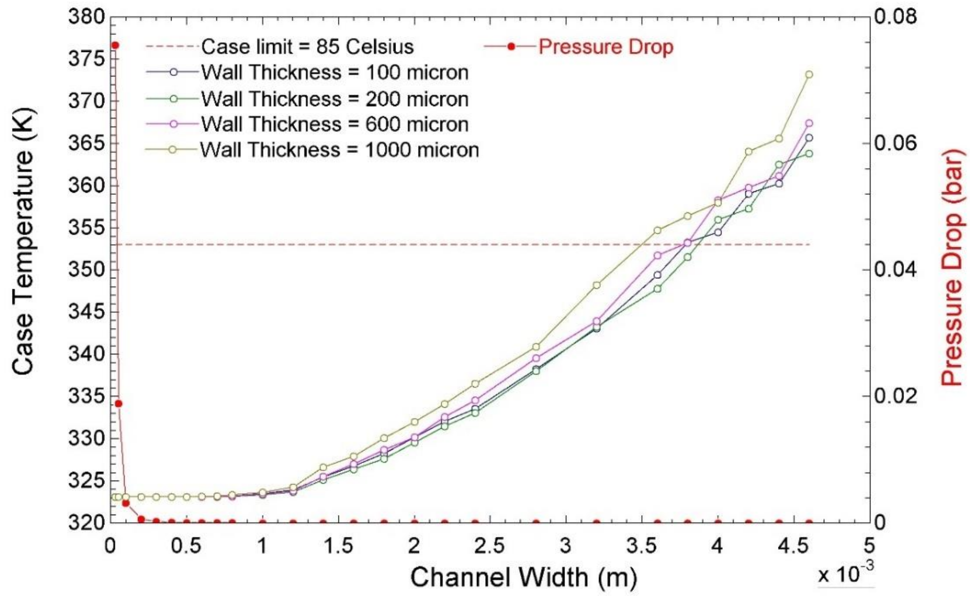

Figure 6: *Plot for Channel Dimensions vs Surface Temperature (bottom side)*

II) Cold plate design using Brass

The brass cold plate design was found with the same analytical methods. Accounting for Manufacuring restrictions and upholding thermal cooling specifications, the cold plate is chosen to be 400-micron wall thickness and 203.2-micron channel width.

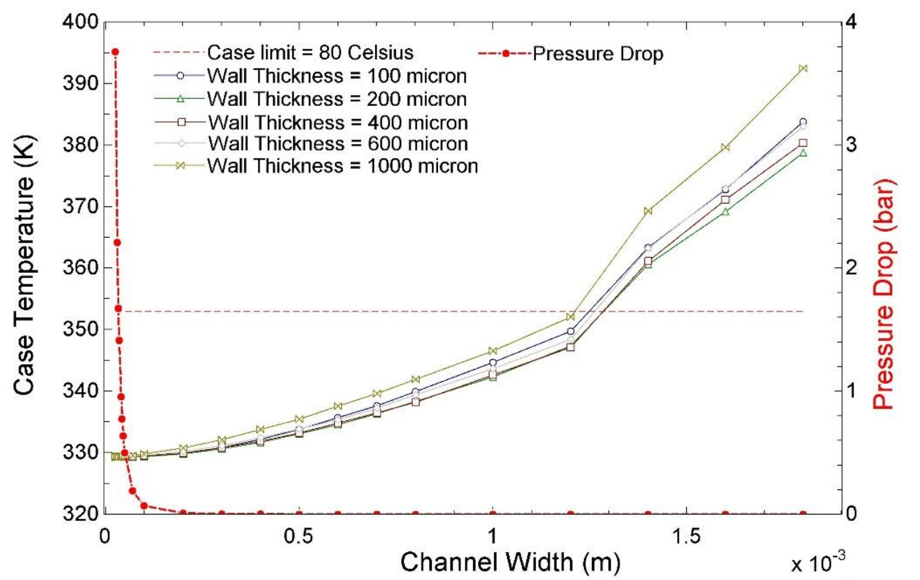

Figure 7: *Plot for Channel Dimensions vs Surface Temperature (top side)*

Simulations of Cold Plate Design

I) Design using Copper

Utilizing this newfound geometry and implemented in Ansys, the following are contours that we simulated using Ansys Fluent:

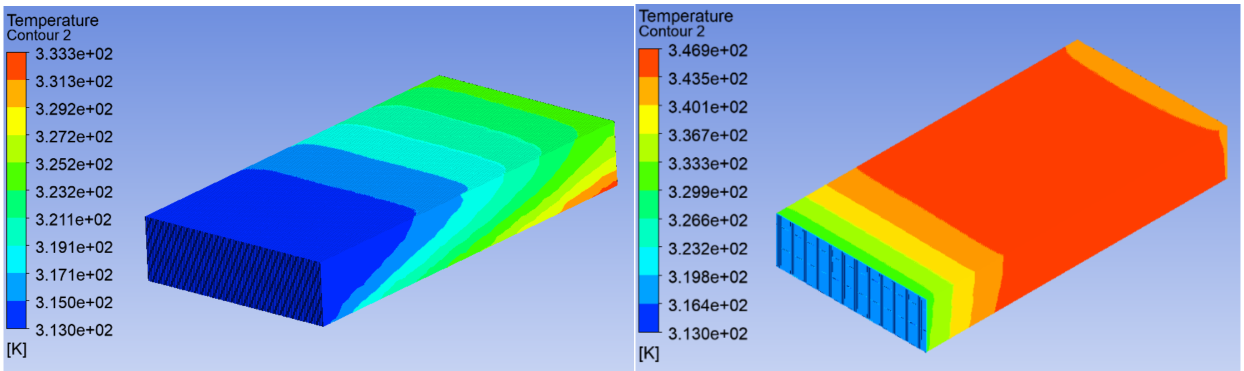

Figure 8: *Frontside (left) and Backside (right) Global Temperature*

In Figure 5, the global temperature for the cold plate stays within our case temperature thresholds for the frontside (80°C) and backside (85°C). The frontside global temperature reaches a maximum of 60.3°C, and the backside global temperature reaches a maximum of 73.9°C.

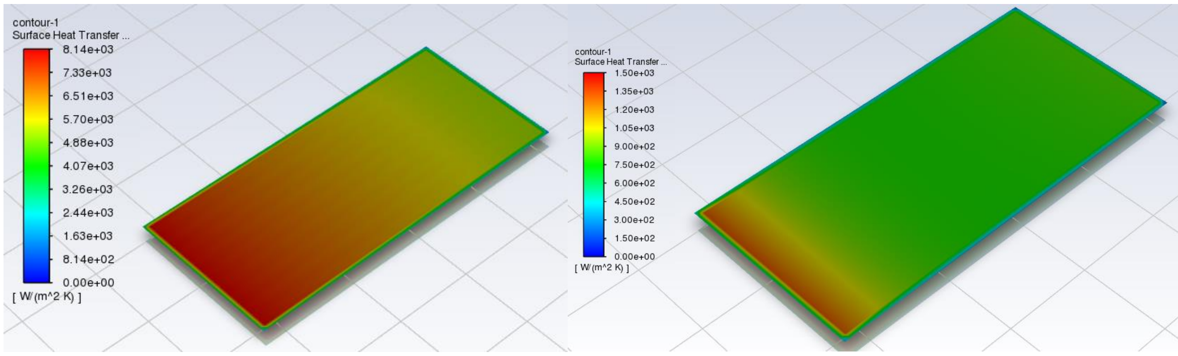

Figure 9: *Frontside (left) and Backside (right) Heat Transfer Coefficient*

As seen in Figure 6, the heat transfer coefficient gradient coincides with the temperature gradient. As the water moves through the channels of the cold plate, it's temperature increases, thus causing the heat transfer coefficient to decrease when our system has a constant heat flux.

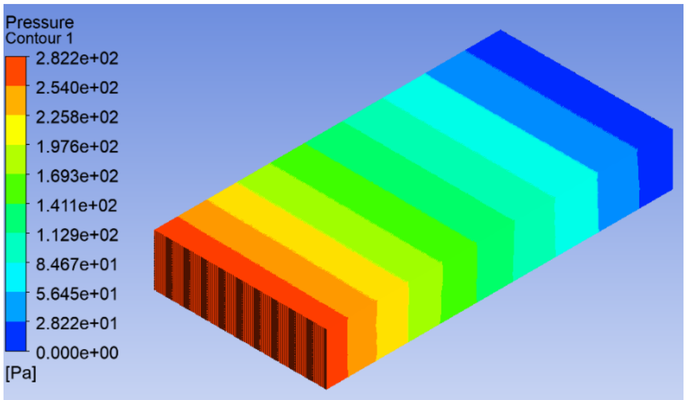

Figure 10: *Pressure Drop (Frontside)*

Our design is well below our pressure drop threshold of ΔP_{max} = 1 Bar(100000Pa). As we can see in Figure 7, our pressure drop result from the simulation was ΔP = 282.2 Pa.

II) Design using Brass

Our team was able to conduct a finite element analysis (FEA) utilizing Ansys Mechanical. Once brass was determined as the final material, FEA helped determine if the cold plate needed additional structural support.

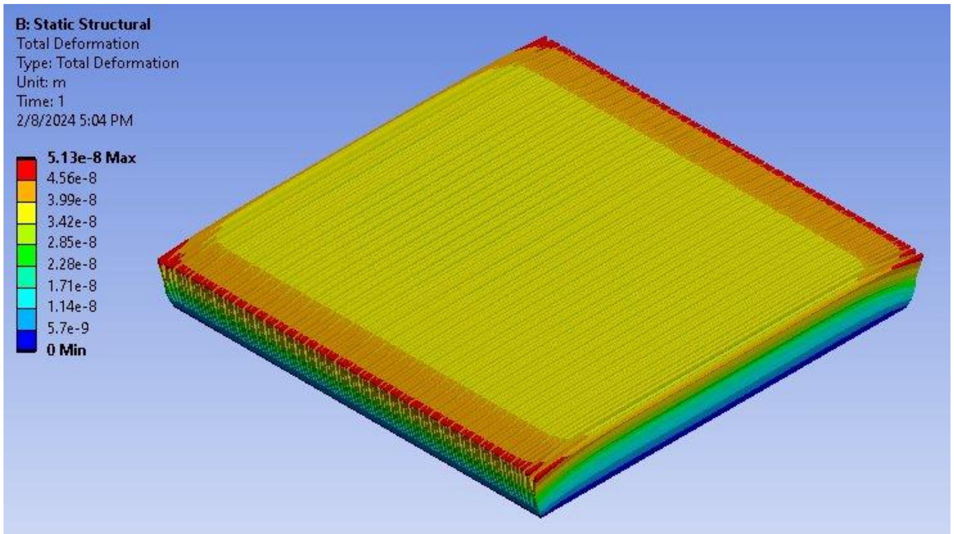

Figure 11: *Total deformation*

It was realized that the outer corners were at risk of crushing from the presented load. Therefore, 4mm walls were created at the cost of a few channels from either side. This caused little effect on the thermal performance of the cold plate. Once this was determined, the mechanical properties of the final cold plate design were analyzed.

Simulations of Cold Plate Mechanical Properties

Mechanical design components are designed to support a pressure of 50 psi so the contact can ensure effective heat removal to the cold plate. Screw holes were implemented to the sides of the cold plate and female screws will be inserted in the holes to apply the pressure. The final design is shown below in Figure 15. Simulations of 50 psi applied can be depicted in Figure 16. The screw holes are located to allow for integration of a housing unit discussed in Chapter 5.

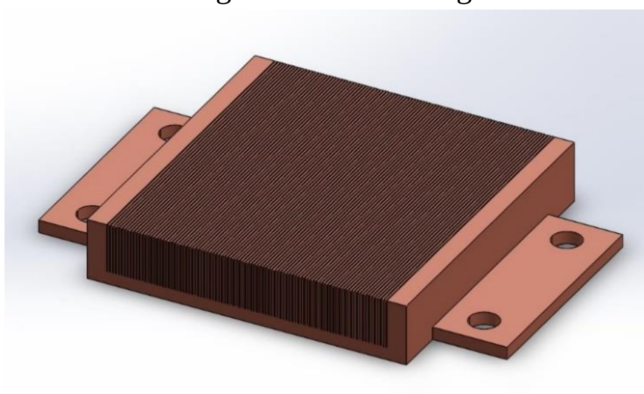

Figure 12: Cold Plate

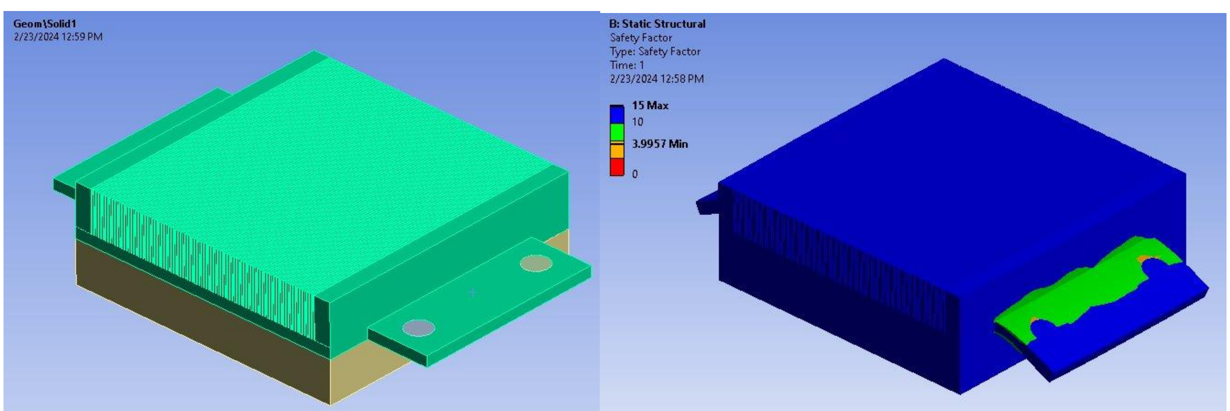

Figure 13: *The Cold plate Model and Heater Block(left) and the Stress Test(right)*

5 Components & Hardware

Figure 14: *Global Testing Apparatus including Voltage Regulator, GFCI, and Cold Plate Assembly. Flow rate is measured through the beaker found in the sink at the outlet pipe.*

Inlet water is controlled in plastic tubing from a laboratory sink. An elbow connector transfer water from the sink to the piping. A control valve and diverting tee allows for control of flow to our desired 1.5 lpm. A beaker and stop-watch are utilized in one outlet of the diverting tee to measure the flow rate as we open the control valve. Experimental results used the flowrate at the outlet of the cold plate. A control valve is inserted before the diverting tee to allow for control of the flow rate. Thermocouple measurements are located at the inlet and outlet of the cold plate and is sealed with epoxy. Water at the end is returned to the sink and measured with a beaker during data collection.

The proposed heater block models a CPU unit that consists of a 1000W heater rod, placed flush in between two brass blocks seen in Figure 14. The two brass blocks are brazed together, and thermal paste ensures the heater is in contact with the brass block maximizing heat transfer.

The brass block is further diverted to the dimensions of the cold plate ensuring more heat is transferred to the cooling system than lost to ambient air. Fiberglass insulation surrounds the heater block to reduce heat loss. It is expected that <5% of heat is lost to the ambient environment. One surface probe thermocouple is inserted into the brass block to measure the temperature of the modeled CPU to ensure the system stays below the desire 80℃ limit. Data collection begins when the surface thermocouple reaches a steady state value.

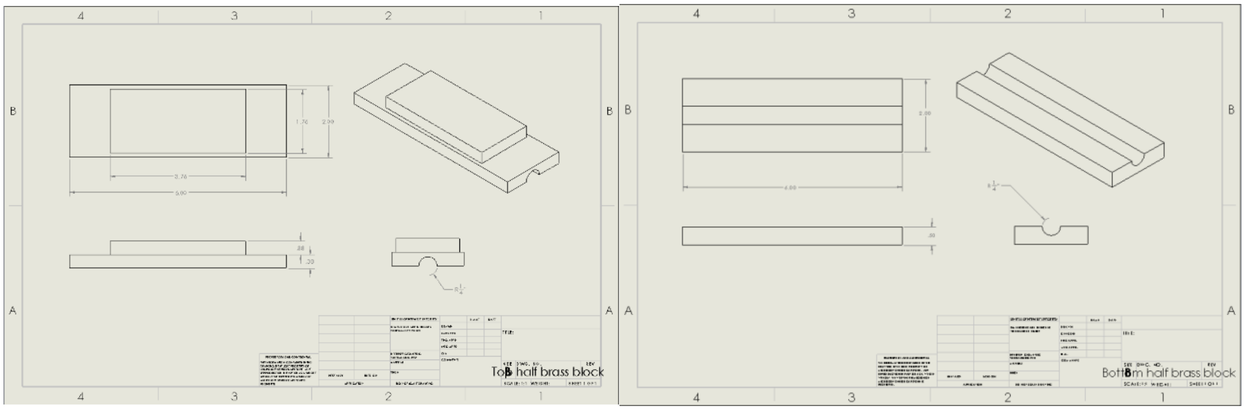

Figure 15: *Engineering Drawings for the Heater Block. A hole is drilled for a thermocouple to be placed in the heater block.*

An Arduino Uno is wired to read measurements from the inlet, outlet, and surface thermocouples using a MAX6675 type K amplifier.

The housing unit of the cold plate is made of polycarbonate and designed to be modular and low-cost allowing for easy disassembly through strew holes. The housing unit covers the top and side surfaces and allows for direct contact of the cold plate with the heater block. Polycarbonate has a thermal conductivity of 0.210 $\frac{W}{mK}$ providing insulation to minimize heat loss. A gasket is placed as an O-ring and on the top surface to prevent water leakage. The housing unit can be depicted in Figure 11.

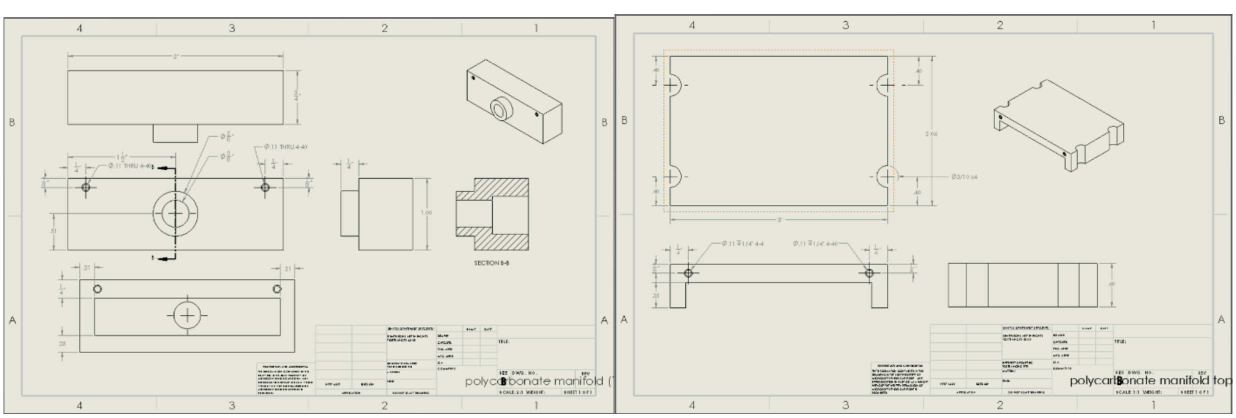

Figure 16: *Engineering Drawings for the Housing Unit. The gasket is placed between the housing unit and the cold plate.*

The cold plate is surrounded by the housing unit and sealed off to allow water to pass thorough without leaking. The top of the cold plate is covered with a gasket as well as the edge of the sides being surrounded by o-rings to prevent leaking. The cold plate is then surrounded by the housing unit which is screwed in to act as a manifold. The area of the cold plate effectively touching the heater block is a 65mm by 65mm area. The assembly of the cold plate, heater block, and housing unit can be seen in Figure 12 and 13.

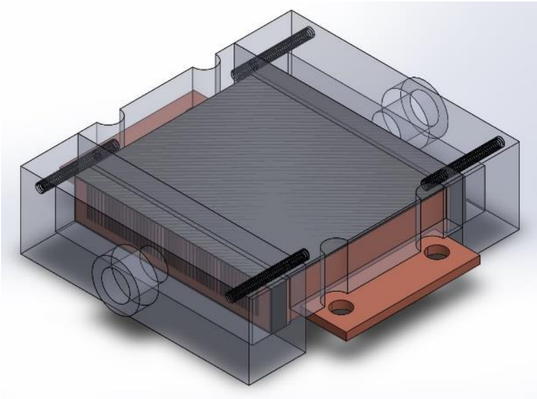

Figure 17: *Cold plate Design with Housing Unit*

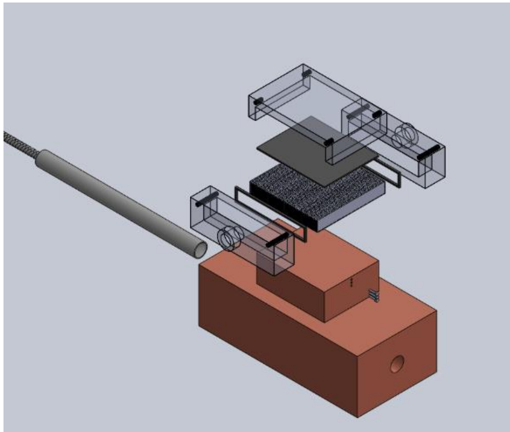

Figure 18: *Exploded view of the modeled 'CPU' heater block, cold plate, and modular housing unit design. A thermocouple is placed in the heater block 5mm from the top surface. Pipes are inserted in the housing unit and a gasket and two O-rings prevent water bypass and leakage.*

6 Testing & Experimentation

Once all materials and equipment was obtained, the setup procedure and initialization could be completed. The following are the steps completed before initial tests were performed:

1) Connect Arduino data acquisition system to a receiving device
2) Connect test system to the sink
3) Turn on faucet
4) Adjust t-valve so that the water flow velocity is around 1.5 lpm using timed measurements
5) Turn diverting t-valve knob so the water flows through the cold plate
6) Turn on the heater inside of the copper block and make sure the heat is set to 1000W
7) Wait until the system reaches steady state.
8) Record the flow rate using the beaker at the outlet and record inlet, outlet, and case thermocouples
9) Regulate power in to an additional 100W
10) Turn off heater and faucet

One full experiment was run where the flowrate was measured first by running the water into a beaker and timing the flow of the water every 200mL. The flow was measured at the outlet piping of the cold plate. A table is shown below for the times and the average flow rate.

Mass Flowrate				
time (s)	volume	volume (liters)	Flowrate (lpm)	mass flowrate mdot (g/s)
10.29	200	0.2	1.166180758	
10.64	200	0.2	1.127819549	
10.71	200	0.2	1.120448179	
10.35	200	0.2	1.15942029	
		AVERAGE	1.143467194	18.90532427

Figure 19: *Table of Average Mass Flow Rate of Water*

After the mass flow rate was measured, the system heater was turned on and official testing had begun. The heater was modulated from 100 to 1000W and the temperature of the inlet, outlet, and case temperature were measured until steady state. Power out is defined as: $P_{out} = \dot{m}c_p(T_i - T_e)$. Adequate heat removed from the cold plate system due to insulation from ambient air is determined by relatively close $P_{in} = P_{out}$. The table for the temperatures as well as the plot for power in vs power out as following:

Power in (watts)	T in	T out	T case	Power out (watts)
104.70	42.25	43.25	46.50	79.40
203.70	43.25	45.50	52.75	178.66
301.80	43.75	47.00	57.50	258.06
401.30	43.50	47.75	62.50	337.46
500.90	40.25	45.75	63.75	436.71
597.40	43.00	49.25	69.25	496.26
713.90	42.75	50.00	72.75	575.67
830.30	42.00	51.00	80.75	714.62
905.40	41.5	52.25	84.75	853.58
1,003.00	40.5	50.5	93	794.02

Figure 20: *Table of Temperatures and Power*

The system is defined as failed state when T_{case} > 80 C. T_{case} is found to supersede 80 C at 830W as seen in Figure 21. In theoretical analysis, T_{case} reaches a maximum of 61 C in Figure 22.

The thermocouples are rated between 32 and 482 C with an uncertainty of 0.75%. A very conservative estimate of uncertainty is 482 (0.0075) = 3.61 C. Further, the 1.5 liter beaker used has an uncertainty of 2.0%. Thus, considering recordings of 1.14 lpm, that is 18.90 g/s, a uncertainty of 0.125 g/s is found. Utilizing the uncertainty equation, $\sigma_f = \sqrt{\left(\frac{df}{d\dot{m}}\right)\sigma_{\dot{m}} + \left(\frac{df}{d\Delta T}\right)\sigma_{\Delta T}}$. In the long form the equation is, $\sigma_f = \sqrt{\frac{\left(\left(\frac{df}{d\dot{m}}\right)\sigma_{\dot{m}} + \left(\frac{df}{dT}\right)\sigma_{T_i}\right)}{\left(\dot{m}\, c_p\, T_i\right)^2}} + \sqrt{\frac{\left(\left(\frac{df}{d\dot{m}}\right)\sigma_{\dot{m}} + \left(\frac{df}{dT}\right)\sigma_{T_o}\right)}{\left(\dot{m}\, c_p\, T_o\right)^2}}$. After simplification by leveraging $\left(\frac{df}{d\dot{m}}\right) = c_p T$ and $\left(\frac{df}{dT}\right) = c_p \dot{m}$, the equation is .$\sigma_f = \sqrt{\frac{\sigma_{\dot{m}}^2}{\dot{m}^2} + \frac{\sigma_{T_i}^2}{T_i^2}} + \sqrt{\frac{\sigma_{\dot{m}}^2}{\dot{m}^2} + \frac{\sigma_{T_o}^2}{T_o^2}}$. After plugging the measured values, the uncertainty of P_{out} = 8.06W.

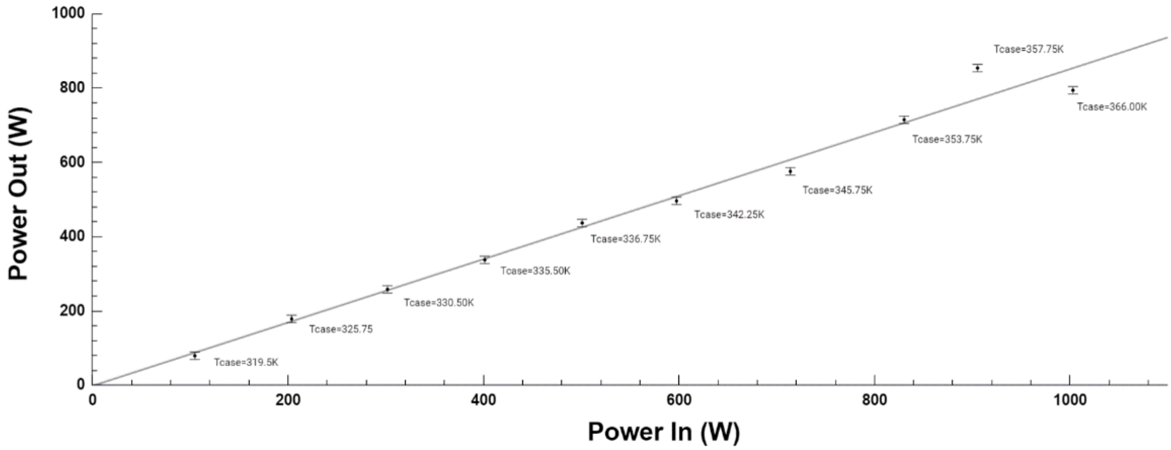

Figure 21: *Experimental results for Power in vs. Power out with the operating case temperature*

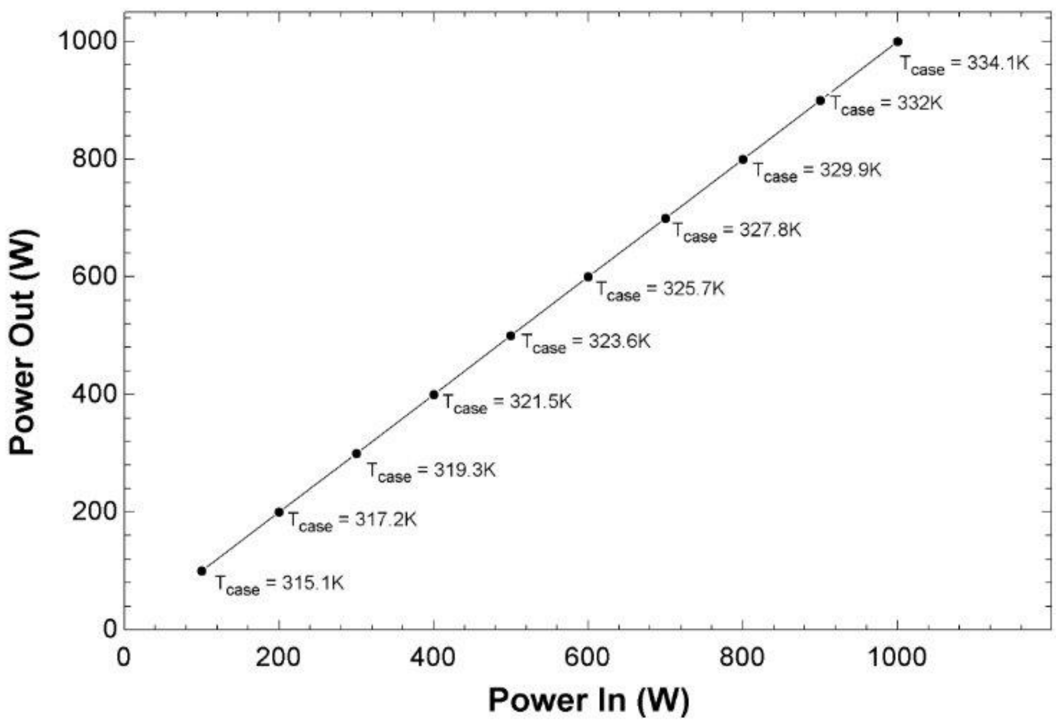

Figure 22: *Theoretical results for Power in vs. Power out with the operating case temperature*

7 Production & Manufacturing & Demonstration

The cold plate was cut using a Computer Numerical Control (CNC) machine. A saw blade is used with the CNC machine to cut the thin channels. The finished channels have metal sheets inserted in them to prevent fin deformation during the cutting of other channels. The final manufactured cold plate is shown below.

The ideal way to manufacture this cold plate is through a process called skiving. This process utilizes a special machine that can cut thin layers out of metal that are then folded up, thus making it a perfect process to produce fins out of copper. However, there were no machines in the SU Machine Shop, so our team resorted to brass material and CNC machining.

Figure 23: *Final Manufactured Cold Plate made from Brass*

Figure 24: *The Ideal Manufacturing Process: a Skiving Machine Folding Copper*

8 Design Assessment

The heat created in the system, Q_{inlet}, is measured from a Watt meter found in Figure 20. A voltage regulator controls a 1000W heater rod. Thermocouple probes measure the water fluid in the inlet and outlet of the cold plate. Limiting the inlet temperature to a maximum 40℃, the heat removed can be calculated as $Q_{water} = \dot{m}c_p(T_e - T_i)$. Conversely, the heat lost to the ambient air is $Q_{air} = Q_{inlet} - Q_{water}$. The percentage of heat lost to ambient air is then found to be $\frac{Q_{air}}{Q_{inlet}} * 100$. If the heat lost to the surrounding air is less than 5%, the system is properly insulated. The surface probe thermocouple in the heater block measures the temperature of the modeled CPU. The experiment must keep the CPU case temperature below 80℃ for a prolonged period of time such that steady state is reached.

Figure 25: *Power meter used to determine the power produced by the cylindrical heater (in watts).*

9 Project Management Timeline

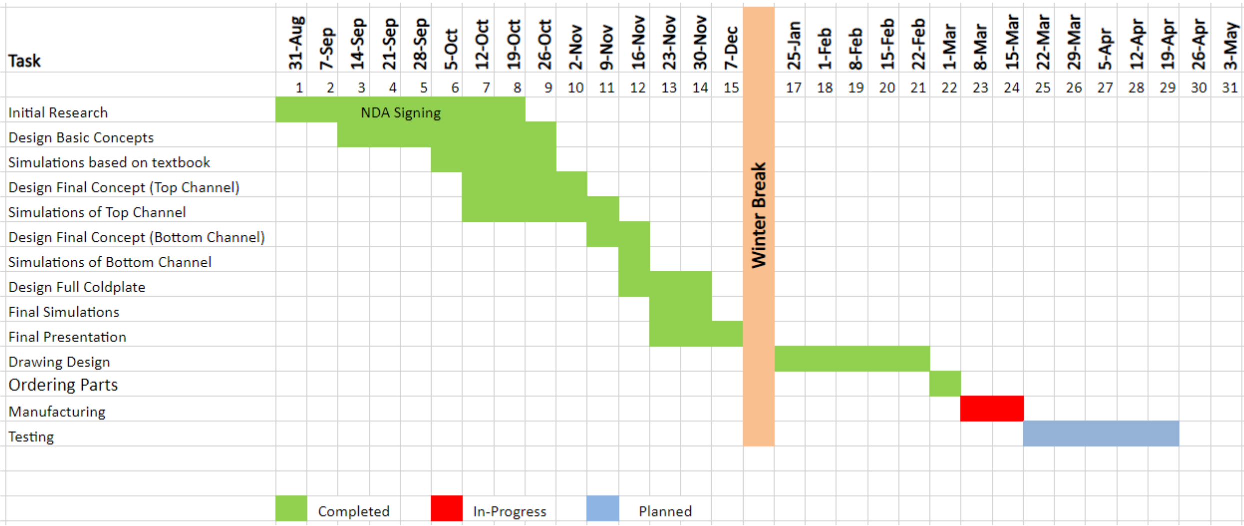

Figure 26: *Gantt Chart of the timeline*

10 Economic Analysis

The purchasing list of the assembly provides an organized materials list. The links to associated parts are seen in liquid Cooled Cold plate Final Report - Syracuse University – Reports – MaterialsList.xlsx file. The system assembly was manufactured with a maximum allotted budget of $1000 USD.

Purchacing List				
Item	Notes	Number of items	Cost per part	Total Cost
Brass block		1	$ 57.45	$ 57.45
		1	$ 93.52	$ 93.52
insertion heater for copper block	0.5 diam, 6 in length, 1000W, get 120V	1	$ 140.77	$ 140.77
Thermocouple for pipes	Type J	3	$ 27.03	$ 81.09
Plastic pipe	6 ft cut into two	1	$ 5.07	$ 5.07
Diverting valve	Works as tee	1	$ 28.46	$ 28.46
Flow valve	control flowrate	1	$ 19.74	$ 19.74
Elbow connector	Sink to plastic pipe	2	$ 6.60	$ 13.20
Arduino MAX6675 connector		1	$ 20.77	$ 20.77
Arduino uno		1	$ 27.60	$ 27.60
Bread board		1	$ 8.99	$ 8.99
Thermal paste		1	$ 5.38	$ 5.38
Gasket	Weather-Resistant EPDM Rubber Sheet, 6" x 6", 1/64" Thic	1	$ 1.36	$ 1.36
Housing unit	SU machine shop materials	2	$ 21.97	$ 43.94
Fiberglass insulation		1	$ 21.00	$ 21.00
Heat sink/ cold plate	Physics machine shop: this parts total cost = 284.65	1	$ 100.66	$ 100.66
		1	$ 60.81	$ 60.81
		5	$ 18.95	$ 94.75
		1	$ 28.43	$ 28.43
Kilowatt reader		1	$ 10.00	$ 10.00
Screws		1	$ 6.35	$ 6.35
Shipping Costs				$ 87.09
Total Cost				$ 956.43

Figure 27: *Materials purchasing list*

11 Societal and Environmental Impact Analysis

The use of water as the liquid of choice for this design is environmentally friendly. Refrigerants, such as R-134a, are being phased out of use for a reason. R-134a is the most abundant hydrofluorocarbon (HCF) in our atmosphere. When used in a closed system, it is safe. However, if there were to be a failure in a cooling system that utilizes refrigerants like R-134a, it would have a detrimental effect on the atmosphere. According to the Environmental Protection Agency (EPA), releasing one gram of R-134a is the same as releasing 1,430 grams of CO2 into our atmosphere.

In addition, the development of a water-cooled heat sink for high powered servers provides increased efficiency to increased computational power demands. As a result, total energy consumption is reduced. Microsoft can expect economic benefit from increased thermal efficiency in the server system. Our problem is very relevant to problems companies are facing today, and our design is solving these problems by having the capability to cool systems with new power requirements while also being environmentally and financially conscious.

12 Conclusions and Future Work

To produce a low-cost cooling system, the system has been tested with a less than ideal efficient thermal efficient material and met budget constraints. Successful experiments using a brass cold plate suggest a copper cold plate with the developed design can meet the constraints and cooling specifications of the system. Given the transition to copper and utilizing the skiving machining technique, special considerations must investigate the material strength and mounting mechanism. Future vibration and fatigue testing ensures mechanical constraints are met and will determine the lifespan of the cold plate but are not expected in the scope of this project. Future design iterations must better account for water leakage.

13 Project and Report Responsibilities

Throughout the year, there have been many responsibilities to split amongst the team. The first semester involved running simulations and research and the second semester involved more simulations and testing. The team's responsibilities for the first semester are shown below.

- Evan Tulsky- Calculations and parametric analysis, and communications lead
- Matthew MacFarlane- Modeling and simulations lead
- Jeremy Kang- Simulations and CAD modeling lead

The team's responsibilities for the second semester are also following.

- Evan Tulsky- Experimentation and communications lead
- Matthew MacFarlane- Simulations lead
- Jeremy Kang- Manufacturing lead

14 References

Çengel, Y. A., & Ghajar, A. J. (2020). *Heat and mass transfer: fundamentals & applications* (6th ed.). Mcgraw-Hill Education.

M. P. David et al., "Experimental characterization of an energy efficient chiller-less data center test facility with warm water cooled servers," 2012 28th Annual IEEE Semiconductor Thermal Measurement and Management Symposium (SEMI-THERM), San Jose, CA, USA, 2012, pp. 232-237, doi: 10.1109/STHERM.2012.6188853.

Roach, J. (2020, September 14). *Microsoft finds underwater datacenters are reliable, practical and use energy sustainably*. Source. https://news.microsoft.com/source/features/sustainability/project-natick-underwater-datacenter/

Song, Z., Zhang, X., & Eriksson, C. (2015). Data Center Energy and Cost Saving Evaluation. *Energy Procedia*, *75*, 1255–1260. https://doi.org/10.1016/j.egypro.2015.07.178

The Weird World Of Liquid Cooling For Datacenters. (2022, June 14). Hackaday. https://hackaday.com/2022/06/14/the-weird-world-of-liquid-cooling-for-datacenters/

Underwater Datacenter Proves To Be A Success. (2020, September 17). Hackaday. https://hackaday.com/2020/09/17/underwater-datacenter-proves-to-be-a-success/

X. Tan et al., "A Novel Cost-Efficient High-Performance Aluminum Cold Plate Solution for Liquid Cooling System," 2022 21st IEEE Intersociety Conference on Thermal and Thermomechanical Phenomena in Electronic Systems (iTherm), San Diego, CA, USA, 2022, pp. 1-4, doi: 10.1109/iTherm54085.2022.9899554.

James, S. M., & Rubenstein, B. A. (2016, May 24). *US9351430B2 - renewable energy based Datacenter Cooling*. Renewable energy based datacenter cooling. https://patents.google.com/patent/US9351430B2/en?q=%28liquid%2Bcooling%2Bsystem%29&oq=liquid%2Bcooling%2Bsystem

H.Y. Zhang, D. Pinjala, T.N. Wong, K.C. Toh, Y.K. Joshi, "Single-phase liquid cooled microchannel heat sink for electronic packages," Applied Thermal Engineering, Volume 25, Issue 10, 2005, Pages 1472-1487, ISSN 1359-4311, https://doi.org/10.1016/j.applthermaleng.2004.09.014.

Srikanth Rangarajan, Scott N. Schiffres, Bahgat Sammakia, "A Review of Recent Developments in "On-Chip" Embedded Cooling Technologies for Heterogeneous Integrated Applications," Engineering, Volume 26, 2023, Pages 185-197, ISSN 2095-8099, https://doi.org/10.1016/j.eng.2022.10.019 .